A Justification for Reflectometers at SNS

John F. Ankner
Spallation Neutron Source Project
Oak Ridge National Laboratory
13 December 1999

SNS document IS-1.1.8.4-6025-RE-A-00

I. Motivation

This past July 15-16, 1999, the Spallation Neutron Source (SNS) Instrument Systems Group presented conceptual designs for instruments at five beam ports to the Instrument Oversight Committee (IOC). One of these concepts described liquids and polarized-beam reflectometers sharing a common beamport [1]. In their evaluation letter [2], the IOC requested that additional information on the capabilities of these instruments be submitted to them before they could recommend further design work. This document addresses these concerns.

The IOC made five specific recommendations concerning the reflectometers. The most important is to develop realistic performance estimates of the proposed reflectometers relative to existing instruments. This topic will be treated in section II below. The other four suggestions, 1) to continue to pursue the multiplexed design, 2) to consider how to provide a wide Q range for kinetic measurements, 3) to explore the possibility of measuring in-plane and plane-normal structures simultaneously, and 4) to consider how to extend the Q range for the liquids reflectometer, do not seem to require such extensive elaboration. These topics are therefore treated together in section III below.

II. Flux Comparison to Existing Reflectometers

II.A. General Considerations

To carry out the flux comparisons in as general and straightforward a manner as possible, I will consider the unpolarized SNS liquids reflectometer. Evaluating the SNS polarized-beam reflectometer is a rather more involved enterprise, but its raw flux should be quite similar to that of the neighboring liquids instrument. Since the IOC meeting in July, I

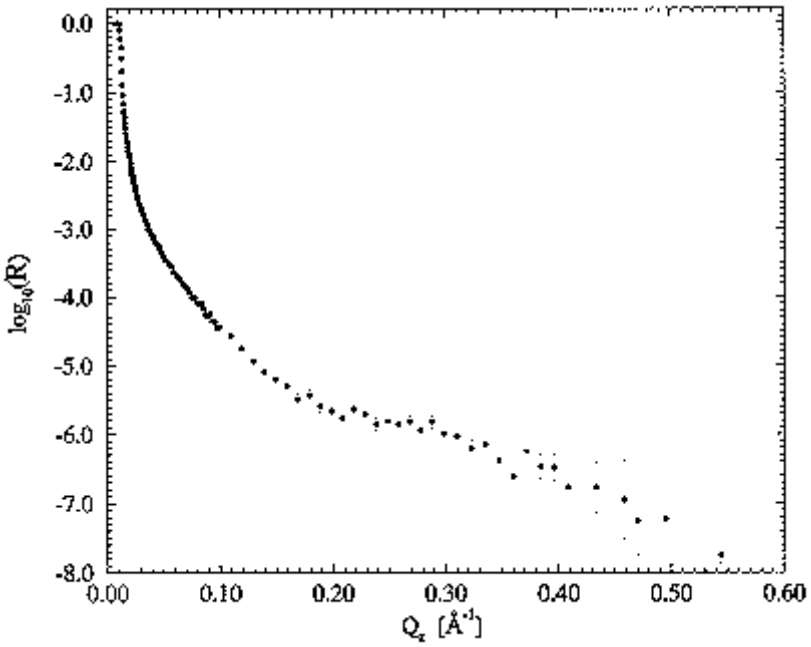

Figure 1: Si reflectivity curve measured at the ADAM reflectometer (from [6]).

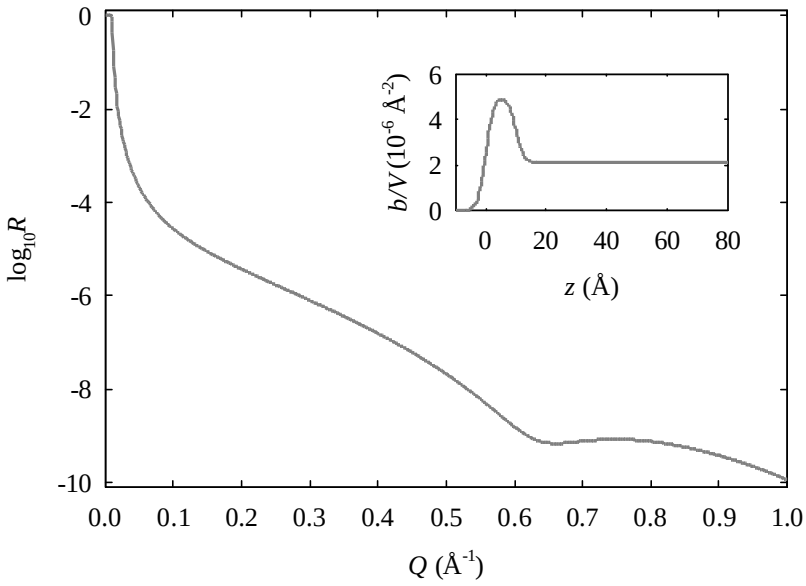

Figure 2: Simulation of ADAM reflectivity data from Fig. 1 extended out to Q = 1 Å^{-1}. The model incorporates a 10-Å-thick oxide layer atop Si.

have refined the design of the liquids reflectometer and presented the results at the Sixth Surface X-Ray and Neutron Scattering Conference [3]. The intensity estimates are carried out by means of the acceptance diagram formalism, an analytical relative of Monte Carlo simulation and ray tracing [4,5].

The silicon wafer clothed in its native oxide layer is the Rosetta Stone of reflectometry. The atomic smoothness and macroscopic flatness required for semiconductor devices satisfy the sample requirements for neutron and x-ray reflectometry as well. Every existing instrument has data on such samples, which are of generally uniform quality, featuring thin oxide layers and low intrinsic background. Figure 1 is reproduced from a paper describing the ADAM reflectometer at the Institut Laue-Langevin [6]. The measured specular reflectivity covers almost eight orders of magnitude at $Q = 0.55\,\text{Å}^{-1}$. One can model the data well by assuming the film to consist of a Si substrate covered by a uniform oxide layer (Fig. 2). The calculated reflectivity of this model can then be used to determine counting times for instruments that have not measured or cannot yet measure the actual sample.

II.B. Count Rate Calculation for the NIST NG-1 Reflectometer

The NIST NG-1 reflectometer shares the same basic design as other vertical-sample fixed-wavelength instruments, such as ADAM at ILL [6] and the Missouri University Research Reactor instrument [7]. Such instruments exhibit the largest dynamic range of existing reflectometers and so constitute the most stringent benchmark for evaluation of SNS performance. At NG-1, a focusing graphite monochromator ($dl / l = 0.015$) diffracts a 4.75-Å beam from the neutron guide through variable-aperture slits onto the sample surface. Specular reflection occurs in a horizontal scattering plane.

When measuring thin layers on large-area samples, one typically increases the slit aperture with increasing angle of incidence q. In this way, one can maintain a constant-area

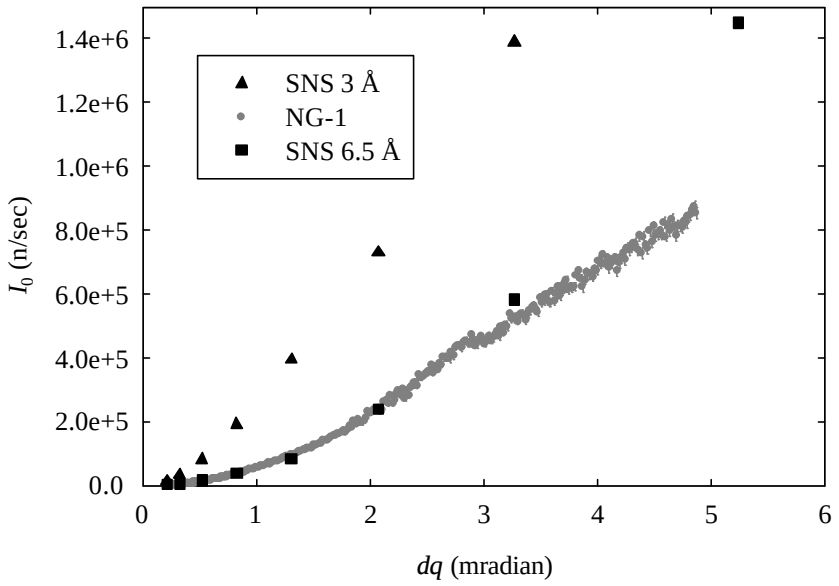

Figure 3: Incident intensity-on-sample of NIST NG-1 reflectometer (l = 4.75 Å) shown in gray, compared with that calculated for SNS liquids reflectometer at 3 and 6.5 Å. For this comparison with NG-1, SNS TOF bins satisfy $d\,l\,/\,l$ = 0.015.

footprint on the surface, increase the intensity-on-sample at large q, and simplify data analysis by holding dq/q constant. The raw data are placed on an absolute reflectivity scale by normalizing to the incident intensity at the various slit apertures. Figure 3 shows such a curve measured with NG-1 (gray circles), in which the slit apertures were varied over $0.03\,\text{cm} \le s \le 0.76\,\text{cm}$ to produce $dq/q = 0.025$.

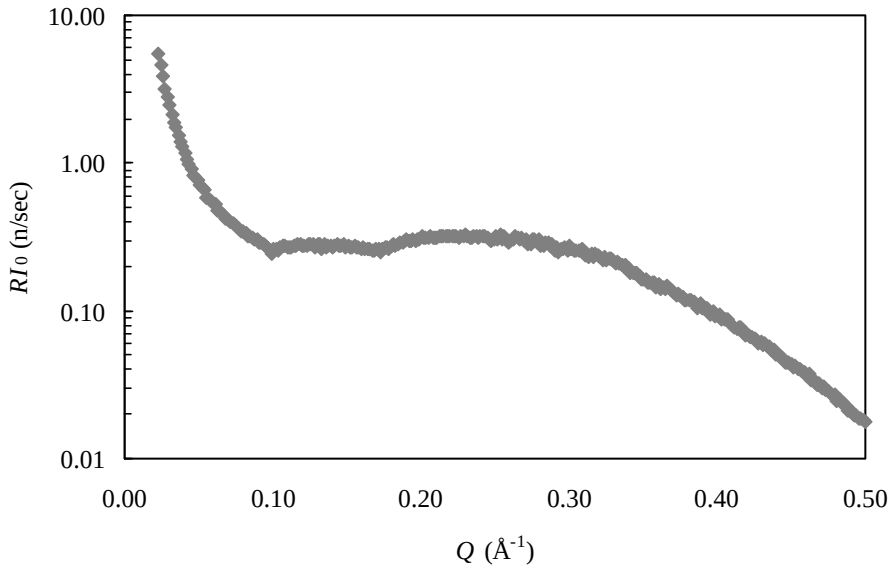

Figure 4: Reflected intensity of "virtual" Si sample determined from measured NIST NG-1 flux.

With a fixed resolution dq/q, each $Q = 4p \sin q / l$ requires a specific value of dq. Simply multiply the aperture intensity curve (Fig. 3) by the model reflectivity (Fig. 2) to obtain the reflected intensity curve shown in Fig. 4. Then, as in an actual experiment, decide how long to count and the necessary ΔQ steps. For these intensity comparisons, I assume 100 counts per Q data point to yield the minimum acceptable statistics and further assume one only counts long enough to accumulate 100 counts per point. As is commonly done, take smaller steps at low Q: for $Q \le 0.1\,\text{Å}^{-1}$, $\Delta Q = 0.0015\,\text{Å}^{-1}$ while for $Q > 0.1\,\text{Å}^{-1}$, $\Delta Q = 0.0075\,\text{Å}^{-1}$.

To determine the time required to collect a complete data set, add the times required to accumulate 100 neutrons (t_{100}) point-by-point (ignoring the time required to move the motors). Figure 5 plots the running sum of the counting times (Σt_{100}) for the scan described above. To measure almost eight orders of magnitude in reflectivity out to $Q = 0.5\,\text{Å}^{-1}$ requires about 65,000 sec or 18 hours, consistent with known instrument performance on actual samples.

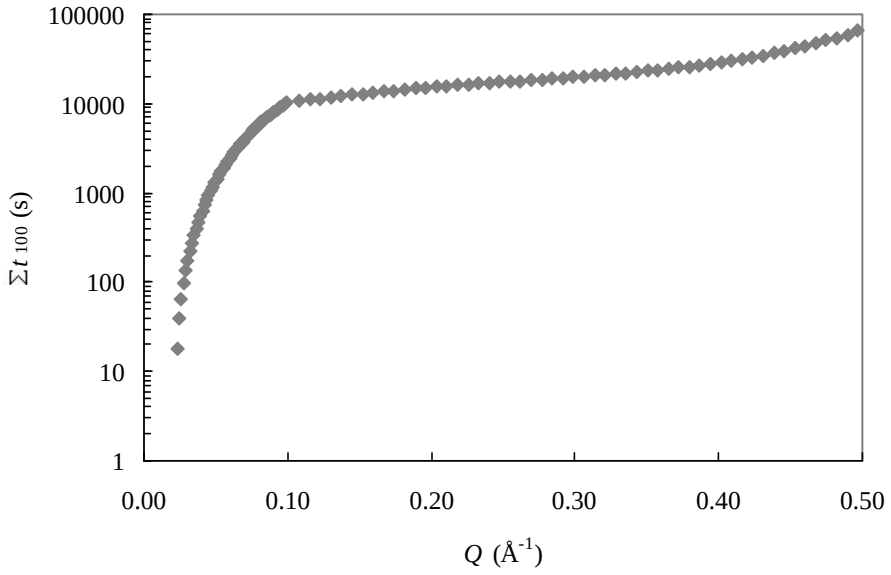

Figure 5: Cumulative counting time (Σt_{100}) to measure Si reflectivity with NG-1.

II.C. Count Rate Calculation for the SNS Liquids Reflectometer

Determining the count rate for a broad-wavelength-band reflectometer is somewhat different than for a fixed-wavelength instrument. In addition, for SNS one does not have actual intensity measurements and so must rely on simulations of the source intensity. Fundamentally, the accuracy of the count estimate depends on the quality of the source simulation, just as the operation of the actual instrument depends on source design and construction. Erik Iverson has carried out extensive Monte Carlo simulations of the different moderators likely to be used at SNS. We plan to place the reflectometers on a beamline that views a partially coupled 20-K super-critical H_2 moderator. Based on

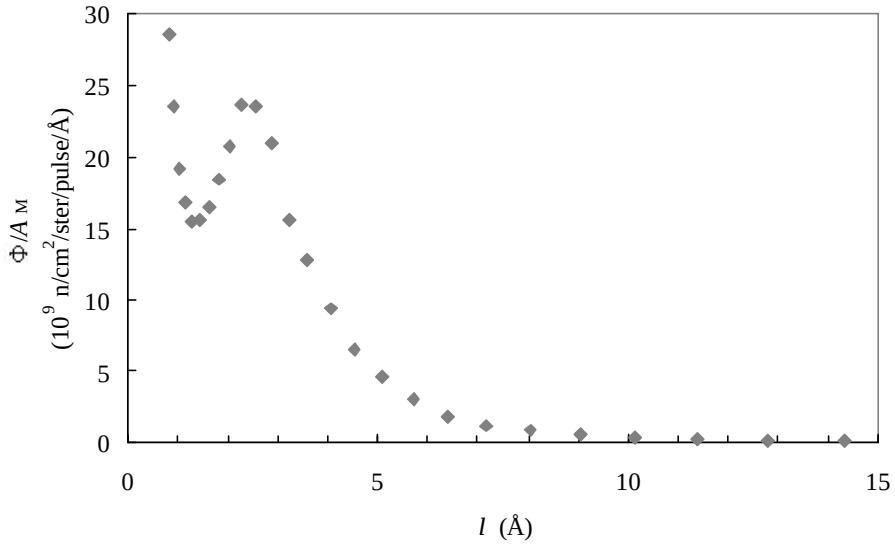

Figure 6: Calculated flux of 2 MW SNS from partially coupled super-critical H_2 moderator at 20 K.

Erik's simulation and assuming the SNS operates at a 2 MW power level, Fig. 6 shows the expected flux as a function of wavelength [8].

The flux units of Fig. 6 reveal the steps needed to calculate count rates. If we specify an aperture area, the solid angular divergence it accepts, the instrument repetition rate, and a wavelength bin size, then multiply these quantities by Φ / A_M ($A_M = 10 \times 12\ \mathrm{cm}^2$ is the area of the moderator face), we obtain incident intensity I_0 in units of n/sec.

The acceptance diagram formalism allows one to specify the spatial and angular dimensions of the optical components that together comprise the reflectometer (see [3] for a more complete description of the instrument shown in Fig. 7). The microguide bender and tapered guide perform two crucial functions in this instrument design: elimination of line-of-sight to the moderator and transport of a large "angular bandwidth" to enable sampling a range of incident angles (again, see [3]).

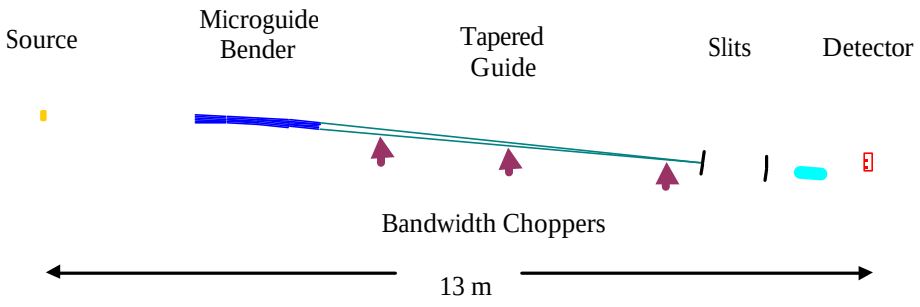

Figure 7: Elevation view of the SNS liquids instrument. The centerline of the tapered guide intersects a liquid sample surface at an angle of 4.75°.

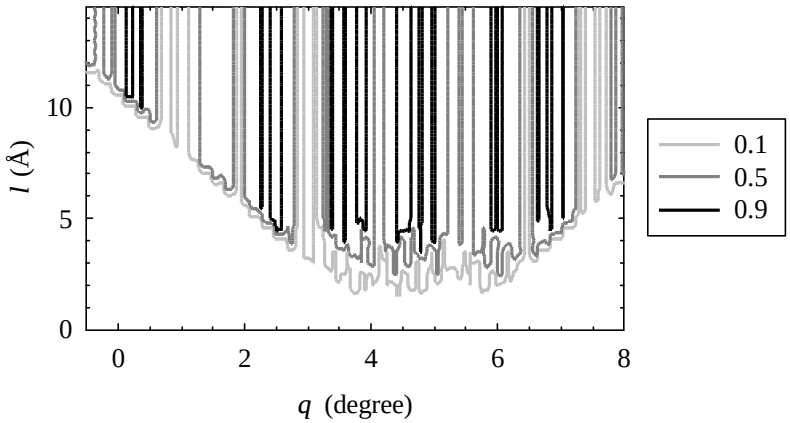

Figure 8: Contour plot of accepted phase area at the exit of the tapered guide. A contour height of 1.0 corresponds to full acceptance of phase space: all flux that can be transmitted through a given aperture is transmitted.

The effectiveness of the optics may be judged by the output of the tapered guide. Ideally, one would like to transport all tolerable angular divergence at all useful wavelengths. For the liquids reflectometer of one's dreams, these parameters might comprise a uniform angular distribution of 10° width containing all $l > 1\text{Å}$. In the real world, by utilizing $4q_c^{\text{Ni}}$ supermirror guide coatings in the bender and tapered guide sections, one can accept the neutron coordinates shown in Fig. 8. The contours represent the fraction of phase space accepted by the guide system in the strongly collimated direction: full illumination (contour 1.0) corresponds to an area of $2\times(4q_c^{\text{Ni}})\times s$, where s is the exit aperture width. On this graph, the ideal situation would be represented by a single 1.0 horizontal contour at $l = 1$, with all longer wavelength neutrons perfectly transported.

As the plot shows, reality is more complicated. There are "dead angles", such as $q = 1.0^\circ$, at which few neutrons are transmitted. Further, due to the limited reflectance of even $4q_c^{\text{Ni}}$ guides, there is not much usable intensity for $l < 3\text{Å}$. Finally, due to the wavelength dependence of the guide coatings, the lower wavelength cutoff increases at angles away from the 4.75° centerline of the tapered guide. Each of these features is the subject of ongoing efforts at optimization. In reference [3], I demonstrated how one might use this imperfect instrument to measure a liquid surface. Below, I apply it to the Si reference sample described above.

Measuring reflection from a solid surface is much simpler than from a liquid surface. Since one can tilt the sample, there is no need to measure intensity off the centerline of the tapered guide. In other words, we can use the most intense portion of the incident spectrum with the broadest wavelength bandwidth. The polarized-beam reflectometer will always operate in this mode.

As stated above, to determine count rates, multiply flux by the appropriate instrumental parameters,

$$I_0(\lambda, dq) = \frac{\Phi(\lambda)}{A_M} X_h(\lambda, dq) X_v(\lambda, dq) \bar{r}^{\bar{m}} f_M \Delta\lambda \,, \qquad (1)$$

where Φ is the integrated moderator flux, A_M the area of the viewed moderator face, X_h the horizontal instrument acceptance (the dimension shown in Fig. 7), X_v the vertical acceptance, $\bar{r}$ the average reflectivity of the guides (assumed 0.9 here), $\bar{m}$ the average number of neutron bounces in the guides, f_M the source frequency, and $\Delta\lambda$ the wavelength channel width. Table 1 shows these parameters in spreadsheet form for $dq = 3.27$ mradian.

The performance of a time-of-flight neutron reflectometer depends crucially on its ability to define the neutron wavelength. Only neutrons in the desired wavelength band, from the appropriate proton pulse, can be allowed to reach the sample. The source repetition rate imposes a fundamental limit on the accessible wavelength bandwidth,

$$\lambda_{max} - \lambda_{min} = \frac{h}{m} \frac{1}{l_{MD} f_M} \,, \qquad (2)$$

where h is Planck's constant, m the neutron mass, l_{MD} the moderator-detector distance, and f_M the source frequency. Every $1/f_M$, the target emits a new batch of neutrons, whose fast members ($\lambda < \lambda_{min}$) overrun the slower neutrons ($\lambda > \lambda_{max}$) of the previous pulse and whose slow neutrons will be caught by the fast neutrons of the succeeding

Table 1: Spreadsheet used to calculate instrument intensity-on-sample with dq = 3.27 mradian (0.188°) for the SNS liquids reflectometer. The parameters are combined according to equation (1) to yield the count rate.

λ (Å)	$f_M\Phi/A$ (n/cm^2/ster/sec/Å)	X_h (radian-cm)	X_v (radian-cm)	$\bar{m}$	$\bar{r}^{\bar{m}}$	$\Delta\lambda$ (Å)	I_0 (n/sec)
1.50	9.552E+11	2.400E-05	5.499E-02	4.58	0.62	0.023	1.75E+04
2.00	1.229E+12	1.190E-04	5.943E-02	3.01	0.73	0.030	1.90E+05
2.50	1.415E+12	1.370E-04	6.393E-02	2.93	0.73	0.038	3.41E+05
3.00	1.126E+12	5.110E-04	6.717E-02	2.10	0.80	0.045	1.39E+06
3.50	8.064E+11	5.290E-04	6.795E-02	2.10	0.80	0.053	1.22E+06
4.00	5.802E+11	5.870E-04	6.795E-02	2.07	0.80	0.060	1.12E+06
4.50	4.026E+11	9.050E-04	6.795E-02	1.97	0.81	0.068	1.36E+06
5.00	2.910E+11	9.950E-04	6.795E-02	1.96	0.81	0.075	1.20E+06
5.50	2.130E+11	9.950E-04	6.795E-02	1.96	0.81	0.083	9.66E+05
6.00	1.542E+11	9.960E-04	6.795E-02	1.96	0.81	0.090	7.64E+05
6.50	1.086E+11	9.960E-04	6.795E-02	1.96	0.81	0.098	5.83E+05
7.00	8.220E+10	9.960E-04	6.795E-02	1.96	0.81	0.105	4.75E+05
7.50	6.540E+10	9.960E-04	6.795E-02	1.96	0.81	0.113	4.05E+05
8.00	5.064E+10	9.960E-04	6.795E-02	1.96	0.81	0.120	3.35E+05
8.50	4.218E+10	9.960E-04	6.795E-02	1.96	0.81	0.128	2.96E+05
9.00	3.432E+10	9.960E-04	6.795E-02	1.96	0.81	0.135	2.55E+05
9.50	2.892E+10	9.960E-04	6.795E-02	1.96	0.81	0.143	2.27E+05
10.00	2.382E+10	9.960E-04	6.795E-02	1.96	0.81	0.150	1.97E+05

pulse. Since wavelength discrimination is achieved via time-of-flight, neutrons from adjacent pulses must be eliminated. The bandwidth choppers perform this function (see Fig. 7). In the current SNS liquids reflectometer conceptual design $l_{MD} = 13\,\text{m}$ and we plan to operate at $f_M = 60\,\text{Hz}$, so our wavelength bandwidth will not exceed 5 Å. In addition, due to enhanced background following emission of the most energetic neutrons, one will commonly utilize wavelength bands that do not overlap a proton pulse: 0.5-5 Å (first frame), 5.5-10 Å (second frame), and 10.5-15 Å (third frame). We are currently optimizing the positions of the bandwidth choppers to provide clean operation in these wavelength bands.

The moderator flux distribution (Fig. 6) dictates that one should operate in the first frame whenever possible to maximize intensity-on-sample. Since the angle of incidence $q \approx lQ/4p$, one requires higher wavelength neutrons only when measuring at high resolution (small dq/q) or for small Q values. Here, our comparison to the NIST NG-1 data can be carried out entirely in the first frame. Recall that the NG-1 reflectometer features $dl/l = 0.015$ and that the data shown in Figs. 3-5 were collected at constant $dq/q = 0.025$. Note from Table 1 that the acceptance of the SNS front-end optics (X_h) only stabilizes for $l \geq 3\,\text{Å}$. Therefore, we will choose q values to cover in $3\,\text{Å} \leq l \leq 5\,\text{Å}$ swaths the same range ($0.022\,\text{Å}^{-1} \leq Q \leq 0.500\,\text{Å}^{-1}$) as the NIST NG-1 measurement described in Section II.B. Table 2 shows the sequence of seven q values needed to span the full Q range. As in the NG-1 measurement, dq/q is held constant at 0.025 and the 3-5 Å wavelength range is broken into bins of width $dl = 0.015 \times l$. The Q points and ranges corresponding to these conditions are shown in Fig. 9, plotted along the calculated specular reflectivity of the model Si sample. The counting times t_{100} are determined by multiplying the model sample reflectivity $R(Q)$ by the intensity-on-sample I_0 to determine the detector count rate (see Table 1),

$$t_{100}(l,q) = \frac{100\,\text{n}}{I_0(l,dq) \times R(l,q)}, \qquad (3)$$

giving the time required to accumulate 100 specularly reflected neutrons in the wavelength bin centered on l (100 counts yielding, in my experience, acceptable statistics).

Table 2: Incident angles required for the SNS liquids reflectometer to duplicate NIST NG-1 performance and the time required (t_{100}) to accumulate 100 counts in the least-intense detector time channel at each incident angle q.

q (°)	dq (°)	l_{min} (Å)	l_{max} (Å)	Q_{min} (Å^{-1})	Q_{max} (Å^{-1})	t_{100} (sec)	Σt_{100} (sec)
0.50	0.013	3.00	5.00	0.0219	0.0366	10	10
0.75	0.019	3.00	5.00	0.0329	0.0548	20	30
1.20	0.030	3.00	5.00	0.0526	0.0877	30	60
1.90	0.048	3.00	5.00	0.0833	0.1389	40	100
3.00	0.075	3.00	5.00	0.1315	0.2192	75	175
4.75	0.119	3.00	5.00	0.2081	0.3469	350	525
7.50	0.188	3.00	5.00	0.3280	0.5467	10000	10525

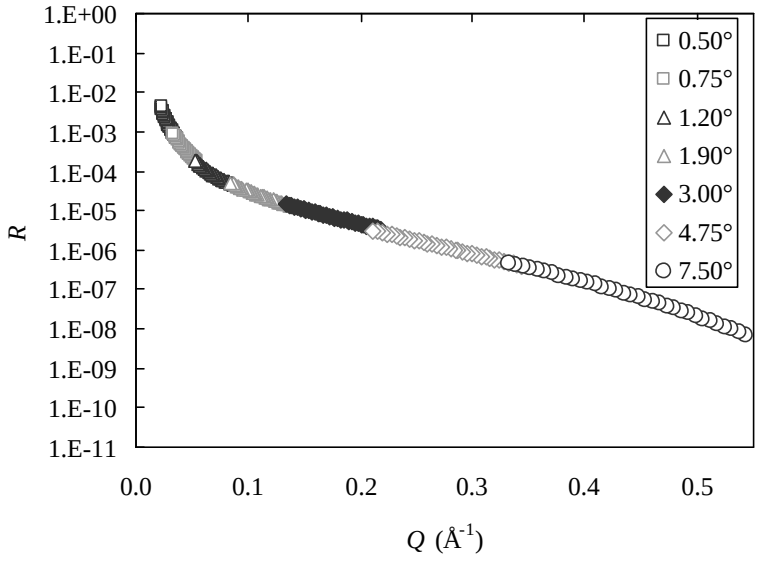

Figure 9: The sequence of incident angles required by the SNS liquids reflectometer to cover a *Q* range out to 0.5 Å^{-1} utilizing a 3-5 Å wavelength band with the same *Q* resolution as the NIST NG-1 measurement.

The largest of these values for each q is listed in the t_{100} column in Table 2, with the cumulative counting times shown in column Σt_{100}. In all measured wavelength bins, counting statistics are equal to or better than those of NG-1, with the error bars being smaller than the symbols.

By the simplest definition of performance, the Si reflectivity measurement that would require 18 hours on NIST NG-1 can be completed in less than 3 hours at the SNS liquids

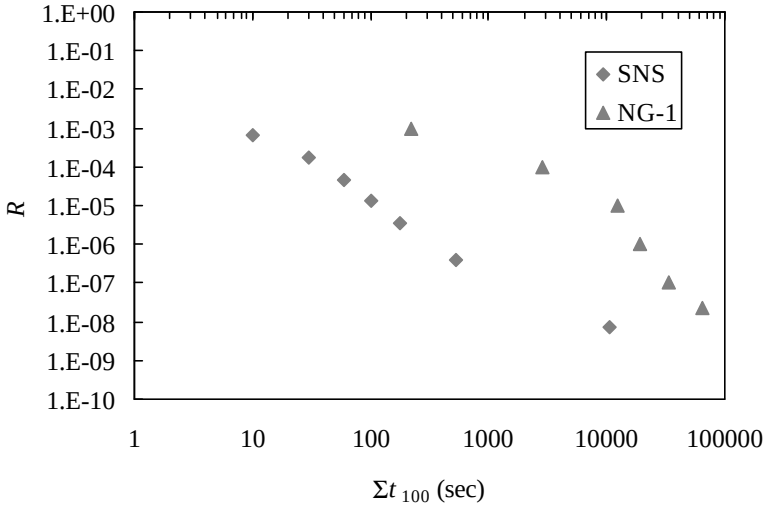

Figure 10: Time required to accumulate 100 reflected neutrons from the model Si film out to a given reflectivity *R*. At all points, the SNS liquids instrument will collect data at least an order of magnitude faster than NG-1.

reflectometer, with identical resolution, to higher Q. A more interesting comparison involves the time required to measure the curve down to a given value of reflectivity (Fig. 10). In such a comparison, the broadband SNS instrument performs better, exceeding the NG-1 data-collection rate by at least a factor of 10 for all R. On the other hand, fixed-wavelength reflectometers excel at collecting data in a narrow Q range, as shown in Fig. 10 by NG-1's improving performance at the longest counting times. The broadband SNS instrument must count long enough for its worst data point, meaning that the other points in that wavelength band have unnecessarily high statistical precision. Figure 3 shows that the monochromatic intensity from the liquids reflectometer viewing a 2 MW SNS at 6.5 Å is comparable to that of NG-1 at 4.75 Å ($dl / l = 0.015$). The NG-1 instrument, placed on an SNS beamline and making no use of time-of-flight, would still marginally outperform the instrument at NIST.

The angular resolution used for the model calculations described above, $dq/q = 0.025$, is excessive. Due to the absence of sharp features in the reflectivity curve, one can obtain an identical fit with much looser angular resolution. Figure 11 shows the sequence of incident angles needed to measure our model Si curve out to $Q = 0.9\ \text{Å}^{-1}$ and $R = 4\times10^{-10}$ at an angular resolution of $dq/q = 0.07$. These data can be collected in less than 5 hours, if we can achieve a 1 n/sec/pixel background level. To be fair, one can also relax the resolution on NG-1. However, the measured intensity of NG-1 (Fig. 3) has begun to deviate from proportionality to $(dq)^2$ by $dq = 5$ mradian. To collect data at $0.9\ \text{Å}^{-1}$ with $4.75\ \text{Å}$ neutrons requires an incident angle of 20° and $dq = 24$ mradian to achieve 7% resolution. The monochromator/guide system on NG-1 will most likely fail to deliver suf-

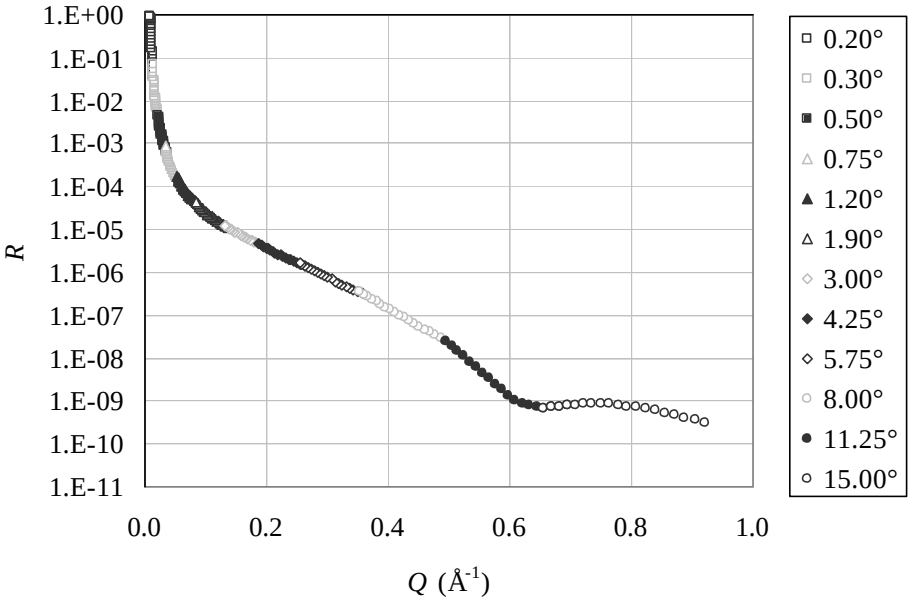

Figure 11: Sequence of incident angles required to measure Si-wafer reflectivity out to $Q = 0.9\ \text{Å}^{-1}$ and $R = 4 \times 10^{-10}$ using 3-5 Å wavelength bands with $dq/q = 0.07$. These data can be collected in 5 hours at SNS.

ficient intensity. Simulations of expected SNS performance indicate proportionality to $(dq)^2$ at least out to the 18 mradian divergence required at $q = 15^\circ$. The efficient transport of flux by the tapered guide yields a tremendous advantage for measurements of very thin layers or any other situation in which one does not require high angular resolution.

II.D. Comparisons to Other Reflectometers

One can roughly evaluate the performance of other reflectometers via the ubiquitous Si wafer, since such measurements are often included in publications describing new instruments. Data collection times are sometimes not given for these scans, although one would assume they are significant, since they serve to showcase instrument performance. Even in the absence of quantitative counting time information, it is interesting to estimate equivalent counting times for SNS.

I reproduced as Fig. 1 a Si reflectivity curve measured on the ILL ADAM reflectometer [6]. Mimicking the smaller $dl / l = 0.006$ of this instrument and assuming $dq / q = 0.07$, the SNS liquids instrument attains $Q = 0.55\,\text{Å}$ and $R = 10^{-8}$ in about 10 minutes. Informal inquiries about the total counting time for the published ADAM curve indicate it was considerably longer. This comparison may be unfair, if the dq / q used for that measurement is significantly less than 0.07. The SNS liquids instrument will in any case be able to measure a comparable data set that quickly.

The SURF instrument at ISIS [9] is the closest existing analog of the proposed SNS liquids reflectometer. It features a vertical specular scattering plane and views a liquid hydrogen moderator illuminated by a 50-Hz spallation neutron source. In contrast to the SNS instrument, it employs a t_0 chopper to reject fast neutrons and gamma rays. By using a chopper rather than a beam bender, SURF can utilize neutrons down to 0.5 Å, compared with the 3-Å cutoff of SNS (SNS should have significantly lower in-beam background due to the greater amount of shielding, however). At a fixed incident angle of $q = 1.5^\circ$, these energetic neutrons enable the study of liquid surfaces out to Q values in excess of $0.5\,\text{Å}^{-1}$. The proposed SNS liquids instrument samples the broad angular output of a tapered guide over $0 < q \le 7^\circ$ with its softer spectrum to achieve a comparable Q coverage [3]. The published SURF Si reflectivity scan (Figure 4 in [9]) spans a bit more than six orders of magnitude in reflectivity. Using $dq / q = 0.07$ and $dl / l = 0.019$, the SNS instrument will be able to collect comparable data in a minute or two. We have undertaken a quantitative investigation of the expected reflectometer background levels – comparison with data from ISIS will no doubt prove fruitful.

For the above comparisons, I have assumed that instrumental background can be held to 1 n/sec/pixel. Such a background level would be considered conservative for a fixed-wavelength instrument, where values a factor of 5-10 lower can be achieved. The harder neutron spectrum of a spallation source and the existence of non-time-correlated delayed neutrons make background reduction a more difficult problem. Failure to achieve these background levels will adversely affect instrument performance, particularly dynamic range. However, the enhanced intensity alone will reduce full-curve data collection times by a factor of 10-100 over the best existing instruments.

III. Other Outstanding Issues

III.A. Status of Multiplexed Design

We have continued to develop the design that places both reflectometers on the same beamport. This design effort has evolved into a proposal to implement wide shutters for multiple-beam extraction on as many as six of the eighteen high-flux-target beamports. The ORNL Target Group and ANL Instrument Group are finalizing a series of Project Change Requests (PCRs) for these and other enhancements to the target monolith. With the added space provided by the wide shutters, one can implement two independent views of the moderator and so not compromise the design of either reflectometer. We must pay careful attention to shielding each instrument from the other. Successful implementation of the multiplexed design remains contingent on installation of a wide shutter. In the unfortunate, and hopefully unlikely, event of project rejection of the wide-shutter PCR, we would recommend that the liquids and polarized reflectometers be constructed on separate beamports.

III.B. Provision of Wide *Q* Range

For many measurements, such as those in which the sample undergoes rapid structural changes, one would like to collect data in a single instrument setting. This capability has long been touted as a design advantage of broadband vs. fixed-wavelength reflectometers. However, even instruments employing a relatively broad wavelength band, such as those at ISIS or IPNS, require two or three incident angles to cover a full Q range at the source frequency.

By dropping pulses, a reflectometer at a high-frequency source, such as ISIS or SNS, can increase its wavelength bandwidth at the cost of a corresponding reduction in intensity [recall eq. (2)]. The ISIS SURF instrument can carry out single-angle measurements at 25 Hz (alternate pulses dropped) because of its hard neutron spectrum ($0.5\,\text{Å} \le l \le 13\,\text{Å}$) [10]. By dropping two of every three pulses at the 60 Hz SNS and using a $3\,\text{Å} \le l \le 15\,\text{Å}$ bandwidth, we will be able to cover the Q range in Table 2 and Figure 9 in two incident angles. Note that the price one pays for the expansion of bandwidth is a factor of three increase in counting time, mitigating the value of this approach for kinetic studies (see Table 3).

We plan to configure the reflectometer chopper systems to accommodate operation at lower repetition rates. The user can then select the appropriate Q range for the experiment. However, due to the intensity cost of dropping pulses, we envision most experiments will be conducted at 60 Hz.

Table 3: Incident angles required for the SNS liquids reflectometer to duplicate NIST NG-1 performance and the time required (t_{100}) to accumulate 100 counts in the least-intense detector time channel at each incident angle q. Two of every three pulses have been dropped so the instrument runs at 20 Hz.

q (°)	dq (°)	l_{min} (Å)	l_{max} (Å)	Q_{min} (Å^{-1})	Q_{max} (Å^{-1})	t_{100} (sec)	Σt_{100} (sec)
1.50	0.038	3.00	15.00	0.0219	0.1096	120	120
7.00	0.175	3.00	15.00	0.1021	0.5105	30000	30120

III.C. Measurement of In-Plane Structures

There are two possible interpretations of the IOC recommendation [2] to investigate measuring in-plane and plane-normal structures simultaneously. First, one can add a detector at large scattering angles to collect Bragg-diffracted intensity from samples mounted on the reflectometer. Alternatively, one can employ a grazing-incidence geometry for depth-sensitive in-plane scattering studies. Current plans call for high-angle diffraction capability to be built into the polarized-beam instrument. Diffraction studies of thin films ($d < 500\,\text{Å}$) are challenging on current triple-axis instruments, so their feasibility on a reflectometer requires careful consideration. Measurement of in-plane structures in grazing-incidence scattering geometries has revolutionized x-ray diffraction. Insufficient flux has so far prevented similar developments with neutrons, although there have been a number of interesting recent experiments. The significantly enhanced intensity of SNS for specular measurements applies as well to conventional, grazing, and off-specular geometries (e.g. grazing-incidence SANS). We have only recently initiated quantitative studies of these geometries, but a simple scaling from existing instruments looks promising.

III.D. High Q Liquids Capability

As stated above, measuring reflectivity from a liquid surface is intrinsically more difficult than studying solid surfaces. Fixed-wavelength reflectometers accomplish this feat by inclination of the monochromator and adjustment of the heights of the slits and sample to vary the angle of incidence. Existing broadband reflectometers at reactors and the instruments at ISIS employ a single incident angle and utilize the largest accessible wavelength band. The 1.5° incident angle used on both ISIS reflectometers, coupled with a hard neutron spectrum ($0.5\,\text{Å} \le l \le 13\,\text{Å}$) reaches wavevectors as large as $Q = 0.5\ \text{Å}^{-1}$. However, these instruments cannot measure $Q < 0.025\,\text{Å}^{-1}$, above the critical angle for external reflection of most materials (e.g. for D_2O, $Q_c = 0.018\,\text{Å}^{-1}$). In the current SNS liquids instrument conceptual design, we can cover $0 < Q \le 0.45\,\text{Å}^{-1}$ by using a softer spectrum and sampling a broad incident angular bandwidth [3].

Sample-generated background ultimately limits the dynamic range of reflectivity measurements. The presence of this background strongly impacts studies involving water. While the 80-barn incoherent cross section of $^1\text{H} \equiv \text{H}$ is well-known, deuterium ($^2\text{H} \equiv \text{D}$) also possesses a significant 2-barn incoherent cross section. Practically, it is difficult to decrease the thickness of a freestanding liquid substrate below about $d = 0.5\,\text{mm}$. For thinner water layers, the solid support distorts the overlying liquid surface, like a pillow under a bedspread [11]. At large angles of incidence, virtually the full intensity of the incident beam I_0 passes through the entire thickness d of the water substrate over its footprint area A, illuminating $N = Ad / v$ atoms ($1/v$ is the atomic number density). Ignoring the Debye-Waller factor, the total incoherent elastic cross section is $(ds / d\Omega)_{\text{inc}} = s_{\text{inc}} N / 4p$, where s_{inc} is the atomic incoherent cross section [12]. We can estimate the count rate using the incident intensities calculated above and the appropriate slit apertures,

$$
\begin{aligned}
I_{\text{inc}} &= \frac{I_0}{A}\left(\frac{ds}{d\Omega}\right)_{\text{inc}}\Delta\Omega = I_0\,\frac{s_{\text{inc}}d}{v}\,\frac{\Delta\Omega}{4p} \\
&= (6.3\times10^{6}\ \text{n/sec})\times\frac{(2\times10^{-24}\ \text{cm}^2)(0.05\ \text{cm})}{1.5\times10^{-23}\ \text{cm}^3}\times\frac{(5.5\times10^{-4}\ \text{ster})}{4p} \\
&= 2\ \text{n/sec.}
\end{aligned}
\qquad (4)
$$

The preceding calculation assumes D_2O is illuminated by $l = 3\,\text{Å}$ neutrons with $q = 5.75^\circ$, $dq/q = 0.07$, $dl/l = 0.019$, and a $5\times1.1\,\text{cm}^2$ detector aperture at 1 m distance. Specular reflectivity $R = 3\times10^{-7}$ produces a comparable signal (see [9], Figure 3 for SURF data from a somewhat thicker D_2O layer).

The existence of sample-dependent background affects instrument design. In general, one cannot measure absolute reflectivities much below the intrinsic background level. For samples containing H, the incoherent background problem increases: for pure H_2O, signal hits background at $R = 1.2\times10^{-5}$. For thin layers atop aqueous solutions, one reaches these limiting reflectivities by $Q \approx 0.4\ \text{Å}^{-1}$, although highly ordered multilayers can produce superlattice peaks at higher Q values. Since reflectivities of 10^{-7} will be collected in a matter of minutes at SNS, we are evaluating the feasibility of using polarized-beam techniques to eliminate the incoherent background [12]. By such means, one could break through the "incoherent barrier".

One can extend the liquid measurement Q range beyond $0.5\ \text{Å}^{-1}$ by using a supermirror-coated multi-channel deflector device (a smaller version of the bender used in the up-front optics) to deflect the incident beam centerline down from its nominal 4.75°. An additional deflection of 2° increases the maximum Q to $0.65\ \text{Å}^{-1}$. Decreasing the incident optics lower-wavelength cutoff from 3 to 2 Å (see Fig. 8) produces even greater benefits: maximum Q becomes $0.77\ \text{Å}^{-1}$. Such a reduction could be achieved through optimization of the deflection angles of the bender and tapered guide and by increasing the length of the instrument (with a corresponding reduction in bandwidth). Incorporating both improvements together increases the liquid measurement maximum Q to $0.98\ \text{Å}^{-1}$. We must carry out a careful cost/benefit analysis of these changes.

IV. Epilogue

We believe that the preceding analysis amply justifies continuing design of the liquids and polarized-beam reflectometers for SNS. Routine reductions of 10-100 in data collection time relative to the best existing instruments alone justify further work. If we can achieve acceptable instrument backgrounds (≤ 1 n/sec/pixel), in ideal circumstances we can extend the Q range of reflectivity measurements beyond $1\ \text{Å}^{-1}$ and nearly close the gap with conventional diffraction. Such a capability would be revolutionary.

References

[1] “Preliminary Conceptual Analysis for a Multiplexed Reflectometry Beamline at SNS,” Frank Klose and John Ankner, SNS Instrument Systems document ES-1.1.8.4-6015-RE-A-00.
[2] Letter to T.E. Mason from D.A. Neumann, 24 August 1999.
[3] “Use of Advanced Neutron Optics in a Liquids Reflectometer,” John F. Ankner, SNS Instrument Systems document IS-1.1.8.2-6021-RE-A-00; Physica B, in press.
[4] J.M. Carpenter and D.F.R. Mildner, Nucl. Instr. and Meth. A **196**, 341 (1982).
[5] J.R.D. Copley, J. Neutron Res. **1**, 21 (1993).
[6] “ADAM, the new reflectometer at the ILL,” A. Schreyer, R. Siebrecht, U. Englisch, U. Pietsch, and H. Zabel, Physica B **248**, 349 (1998).
[7] H. Kaiser, K. Hamacher, R. Kulasekere, W.-T. Lee, J.F. Ankner, B. DeFacio, P. Miceli, and D.L. Worcester, in *Inverse Optics III*, SPIE Proceedings Vol. 2241 (Society of Photo-Optical Instrumentation Engineers, Bellingham, Washington, 1994), pp. 78-89.
[8] E.B. Iverson, private communication.
[9] “SURF – A Second Generation Neutron Reflectometer,” D.G. Bucknall, J. Penfold, J.R.P. Webster, A. Zarbakhsh, R.M. Richardson, A. Rennie, J.S. Higgins, R.A.L. Jones, P. Fletcher, R.K. Thomas, S. Roser, and E. Dickinson, in *ICANS-XIII*, edited by G.S. Bauer and R. Bercher (Paul Scherrer Institut, Villigen, Switzerland, 1995), pp. 123-29.
[10] See www.isis.rl.ac.uk/largescale/SURF/technical/Tech_Spec.htm for the instrument parameters.
[11] M.D. Foster, private communication.
[12] *Thermal Neutron Scattering*, G.L. Squires (Cambridge University Press, New York, 1978).